

# Extraction of pores from microtomographic reconstructions of intact soil aggregates

Paul B. Albee\*  
Computer Science and Eng.  
Michigan State University  
East Lansing, MI 48824

George C. Stockman  
Computer Science and Eng.  
Michigan State University  
East Lansing, MI 48824

Alvin J.M. Smucker  
Crop and Soil Science  
Michigan State University  
East Lansing, MI 48824

## Abstract

Segmentation of features is often a necessary step in the analysis of volumetric data. We have developed a simple technique for extracting voids from a irregular volumetric data sets. In this work we look at extracting pores from soil aggregates. First we identify a threshold that gives good separability of the object from the background. We then segment the object, and perform connected components analysis on the pores within the object. Using our technique pores that break break the surface can be segmented along with pores completely contained in the initially segmented object.

## 1 Introduction

The objective of this research is to segment the pores, or voids, from an object imaged in three dimensions by x-ray microtomography. One area of application is soil science. The pores between particle arrangements within soil aggregates modify convective-dispersive flow of inorganics, organics, and radionuclotides through soil. The flow and uptake of materials through these pores within aggregates determine how well plants will grow [1]. Techniques such as Marching Cubes [2] can be used to extract the surface of the pores, but do not handle surface-breaking pores. Surface breaking pores produce concavities in the surface, raising the question of where the pore terminates. These pores are interesting since they provide information about voids in the object rather than the object itself. We propose a technique that preserves surface breaking pores, and clearly identifies the location and termination of individual pores.

## 2 Experimental Apparatus

We used a rotating microtomographic apparatus to acquire soil aggregate data which was collected at the

GSECARS<sup>1</sup> beamline at the Advanced Photon Source (APS) at Argonne National Laboratories. The experimental setup is shown in Figure 1. The x-ray source is a 7 GeV synchrotron, which produces an x-ray beam by a bending magnet. The appropriate energy was selected from the white beam using the monochromator. This microtomographic experiment was run at 20 KeV. Soil aggregates being scanned were positioned in the beam between the monochromator and the scintillator. The camera, a Princeton Instruments Pentamax with a Kodak 1035 × 1317 CCD, then acquired three hundred sixty projections of each aggregate onto the scintillator as the object was rotated. Once all of the data was collected, a three dimensional volume model was reconstructed using filtered back projection [3].

## 3 Algorithm

The input is an  $n$ -level volume where  $n$  is some number greater than 1. The volume is assumed to broken into two broad classes, object and background. It is assumed that the grey-level distribution is approximated by a bi-modal Gaussian, Figure 2. We extract the object from the volume, and then isolate and analyze the voids in the object.

The major steps in the pore extraction algorithm are given below.

1. Automatic Threshold Determination
2. Extract Aggregate From Background
3. Pore Identification
4. Connected Components [4] on Pores
5. Label Components

---

\*Guest Graduate, Argonne National Laboratory, Argonne, IL, 60439

---

<sup>1</sup>Geological Soil Environmental Coalition for Advanced Radiation Sources

### 3.1 Automatic Threshold Determination

In order to segment the aggregate from the surrounding air a threshold is used. A global threshold is used to clip out the entire volume.

The first derivative is computed and used to identify maximas and minimas in the histogram. The two largest local maximas are identified. The threshold is then set to the intensity with the fewest counts between the maximas. If the actual data is well approximated by the assumption of a bi-modal Gaussian distribution, then the threshold will be the smallest minima between the maximas, Figure 3.

### 3.2 Extract Aggregate From Background

The aggregate is extracted from the background in order to define a boundary for surface breaking pores. The boundary of the aggregate is determined using a convex hull on a per slice basis. Areas outside of the hull are indicated using a sentinel value.

The initial separation of the soil aggregate from the background is done by thresholding a median filtered version of the slice. This thresholding produces a binary image of the aggregate and some noise in the air around the aggregate. Erosion and dilation operations are then applied to the binary image to remove the noise in the air region. A *Roberts* edge detector is then applied to the cleaned image. The points from the edge detector are then used to construct a convex hull.

Once the hull has been constructed, all points outside of the hull are labeled with a sentinel value to indicate they are not part of the soil aggregate.

The input image is shown in Figure 4a, and the segmented image is shown in Figure 4b. Note that there are air spaces around the edges of the aggregate in the segmented image. These spaces may correspond to either surface breaking pores or concavities in the surface of the soil aggregate.

Once all of the slices are processed, they are recombined to generate the segmented soil aggregate volume.

### 3.3 Pore Identification

Once the aggregate has been segmented from the background the pores may be identified via a bandpass operation. The sentinel value is the smallest value that can be represented for a given data type. The pores are those regions whose intensity value is between the sentinel and threshold values determined for each slice. A binary image of the pores is generated by setting all pixels whose intensity is between the sentinel and threshold to 1, and all other values to 0. In three dimensions this generates a binary representation of all pores in the soil aggregate.

Feature	Theoretical	Measured	Error %
Sphere	4189	4112	1.83
Tube	20944	20277	3.18

Table 1: Sizes of pores in phantom in voxels.

### 3.4 Pore Labeling

Once the pores have been segmented they are labeled for future analysis. Labeling is accomplished through a three dimensional connected components analysis. All adjacent voxels that are within a pore are marked as belonging to the same pore. The resulting labels then correspond to the order of discovery of the pores by the connected components algorithm. After the pores have been identified, volume, diameter, and other features can be computed for each pore.

## 4 Results

We show results on two data sets, Figures 6 and 4. The first data set is a numerical phantom, Figure 6, while the second is a soil aggregate from Kenya, Figure 4.

The phantom is a sphere with a radius of sixty voxels. A ten voxel sphere has been removed from the phantom as well as a tube with radius ten. Once the phantom was constructed, normally distributed noise was added to simulate sensing and reconstruction error. The histogram for the phantom is shown in Figure 5. A slice of the phantom is shown in Figure 6a. In Figure 6b the phantom has been segmented from the background. The extracted pores are shown in Figure 6c. The sizes of the detected pores in the phantom are given in Table 1. The larger error for the tube is due to the tube breaking the surface of the aggregate, and the tube's larger surface area proportional to its volume.

We have also run our algorithm on a topographic reconstruction of a soil aggregate from Kenya. An input image is shown in Figure 4a. Note the outer edge of the soil aggregate is irregular. Figure 4b shows the slice after the aggregate has been segmented. The surface breaking pores are now shown. Shown in Figure 4c are large pores in a soil aggregate from Kenya. The light areas in the image represent pores in the soil aggregate, while the black area corresponds to the actual soil aggregate and surrounding air. All pores smaller than 2000 voxels were not rendered. The diagonal strip across that center of the image is a pore that goes through the center of the aggregate. The flat area on the right side of the image is where a surface breaking pore was terminated by our algorithm. The separated pores on the left side of the image are

relatively small, in the range of 2000 – 3000 voxels.

Shown in Table 2 are the volumes and centroids for all pores in Figure 4c greater than 2000 voxels. The very large pores in the Kenya soil aggregate are surface breaking pores.

## 5 Concluding Discussions

We are able to extract pores from a volumetric data set with our algorithm. The algorithm outlined is relatively simple, and is applicable to segmenting objects where there are no assumptions other than that the object is separable from the background via thresholding. Future work on this algorithm involves improving the segmentation procedures for the soil aggregate. The convex hull may identify regions on the surface of the aggregate that do not correspond to actual pores. Currently being explored is the use on non-convex hulls, particularly energy minimizing splines.

## 6 Acknowledgements

This work is supported in part by the U.S. Department of Energy, Basic Energy Sciences, Office of Energy Research, under contract W-31-109-ENG-38, the Mathematical, Information, and Computational Sciences Division subprogram of the Office of Advanced Scientific Computing Research, under Contract W-31-109-Eng-38, the U.S. Department of Agriculture under contract USDA/NRI 97-35107-4322, and GeoSoilEnviroCARS: A National Resource for Earth, Planetary, Soil and Environmental Science Research at the APS, under contracts Department of Energy — Geosciences(DOE DE-FG02-94ER14466) and National Science Foundation - Earth Sciences(NSF EAR-9906456).

## References

- [1] W. A. Jury and K. Roth, *Transfer Functions and Solute Movements through Soils. Theory and Applications*, Birkhäuser Verlag, Basel, Switzerland, 1990.
- [2] William E. Lorensen and Harvey E. Cline, “Marching cubes: A high resolution 3D surface construction algorithm,” in *Computer Graphics (SIGGRAPH ’87 Proceedings)*, Maureen C. Stone, Ed., July 1987, vol. 21, pp. 163–169.
- [3] Gabor T. Herman, *Image reconstruction from projections: the fundamentals of computerized tomography*, Academic Press, 1980.
- [4] D. H. Ballard and C. M. Brown, *Computer Vision*, Prentice-Hall, 1982.

Pore		
Volume	Centroid	Surface Area
989119	(203.3, 243.3, 163.4, )	405078
548577	(271.2, 205.3, 359.7, )	252646
353981	(466.1, 266.5, 181.8, )	114082
221925	(293.7, 351.0, 224.9, )	60956
86243	(371.3, 431.5, 139.1, )	38884
62347	(340.8, 122.7, 152.0, )	44924
35183	(155.0, 407.7, 310.6, )	21698
26259	(473.2, 138.2, 229.3, )	14516
25469	(254.5, 244.8, 211.3, )	14106
24929	(431.2, 317.5, 190.1, )	10656
17677	(408.9, 402.8, 233.0, )	14208
14013	(256.9, 240.5, 273.6, )	13878
10968	(238.9, 452.2, 139.8, )	10600
9382	(266.8, 178.0, 211.4, )	4918
7792	(148.8, 430.0, 167.9, )	4804
6465	(404.2, 279.5, 220.5, )	6054
5163	(207.8, 196.8, 323.6, )	3678
5085	(368.7, 92.3, 362.4, )	5954
5003	(263.1, 264.8, 249.8, )	5300
4540	(178.5, 360.8, 348.1, )	3584
4447	(115.9, 177.7, 351.6, )	4570
4363	(247.2, 128.5, 201.9, )	4696
3541	(274.3, 283.1, 166.4, )	5148
3422	(92.8, 360.1, 310.6, )	2782
3092	(327.0, 327.9, 126.4, )	2606
2880	(390.4, 356.7, 216.8, )	2916
2652	(254.7, 120.2, 286.3, )	2838
2596	(433.1, 157.0, 192.1, )	2200
2553	(163.3, 111.1, 302.4, )	2668
2533	(450.7, 122.6, 298.7, )	2908
2400	(412.4, 338.2, 288.8, )	4074
2248	(125.4, 269.3, 402.9, )	3326
2208	(301.0, 218.4, 384.5, )	1790
2198	(340.4, 231.7, 278.8, )	1828
2124	(348.1, 417.4, 223.0, )	2078
2111	(387.8, 58.8, 302.2, )	2510
2035	(130.9, 326.1, 224.1, )	1354

Table 2: Pore features from Kenya soil aggregate. Each voxel is approximately 131 cubic microns

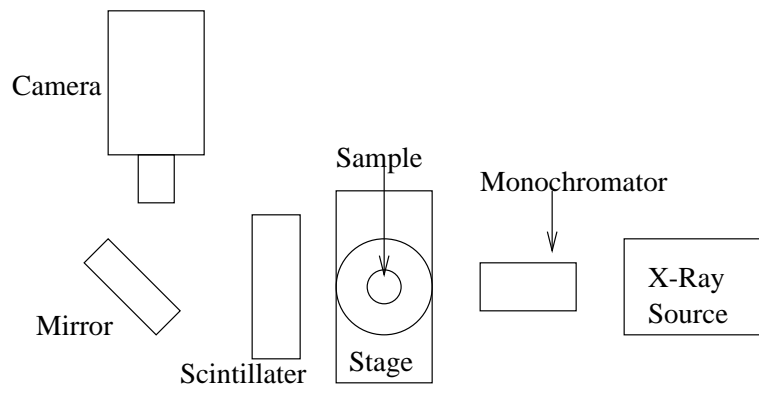


Figure 1: Microtomographic Experimental Setup

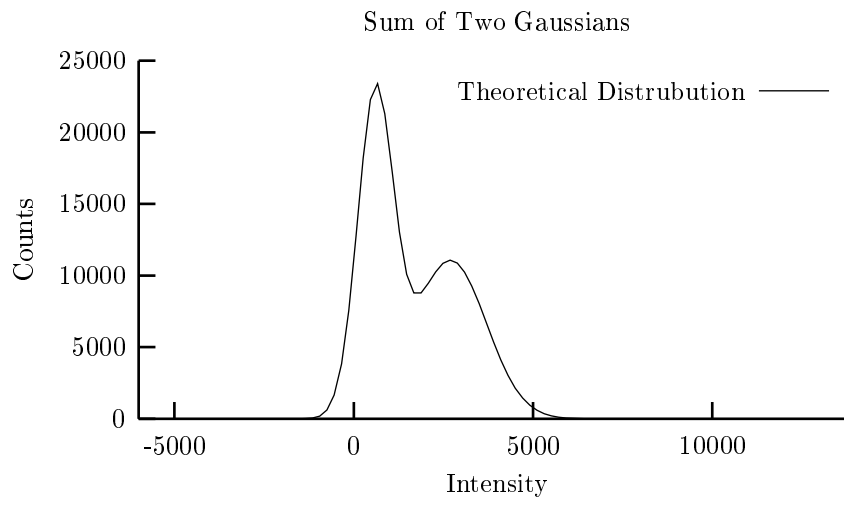


Figure 2: Sum of Two Gaussians

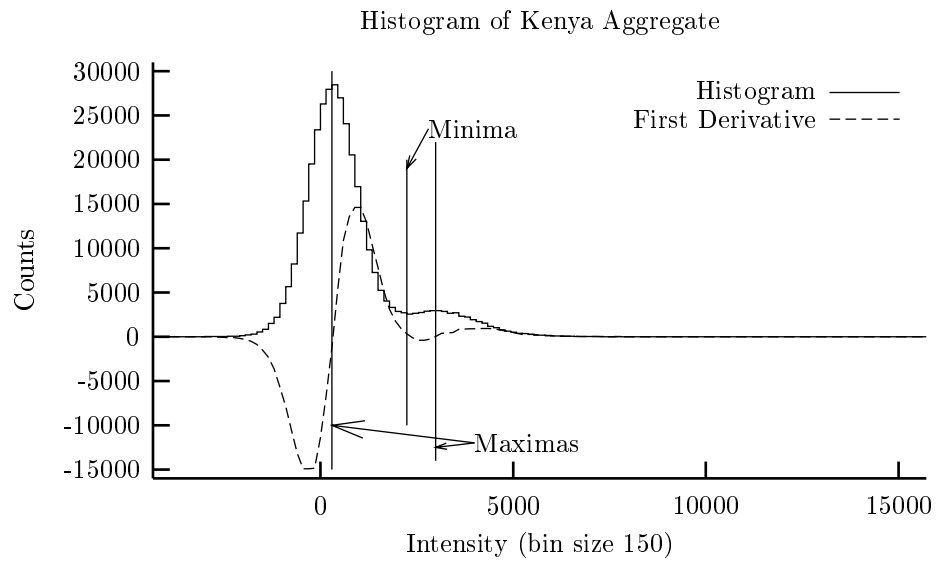
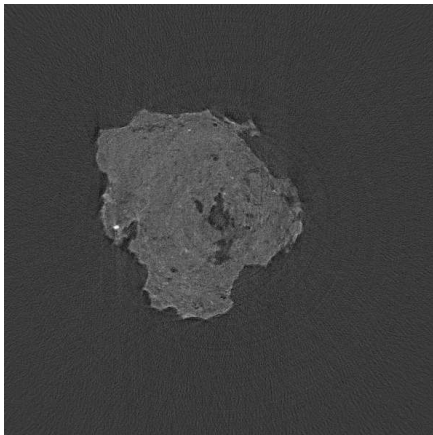
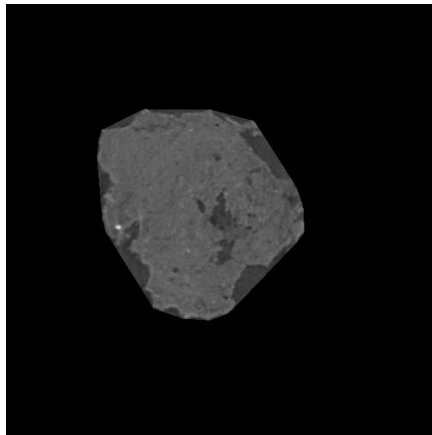


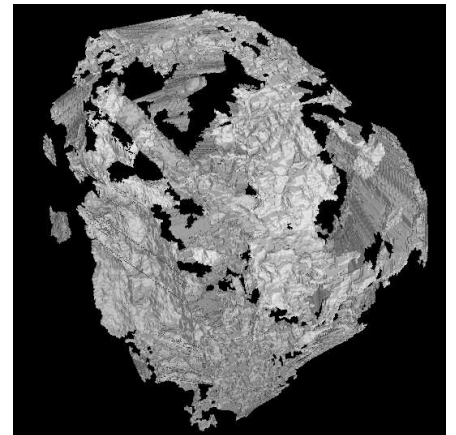
Figure 3: Real Data



(a) — Input



(b) — Segmented



(c) — Extracted Pores

Figure 4: Aggregate Data

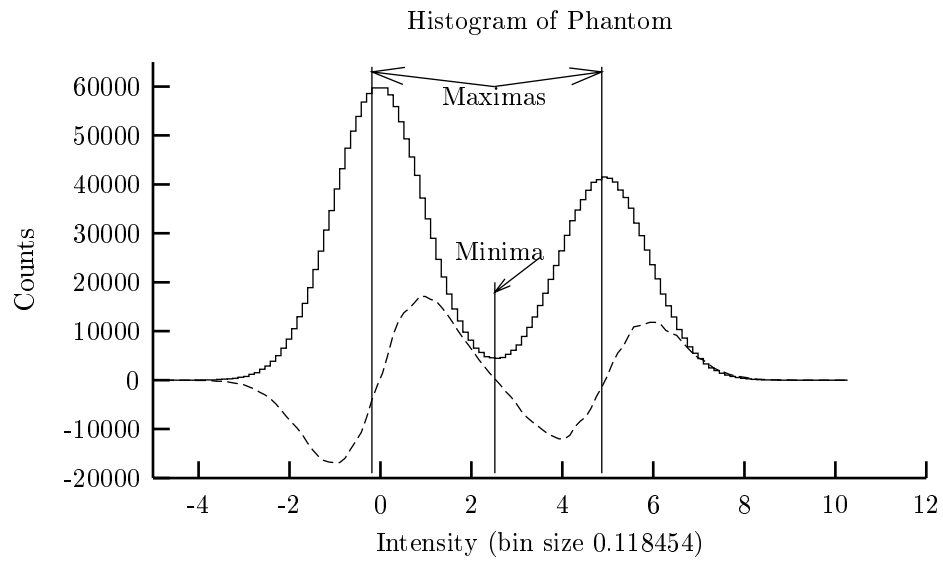


Figure 5: Phantom Histogram

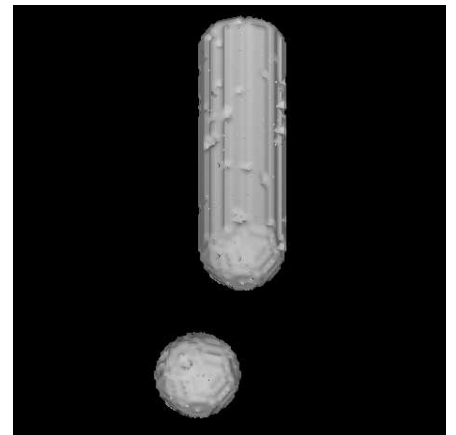
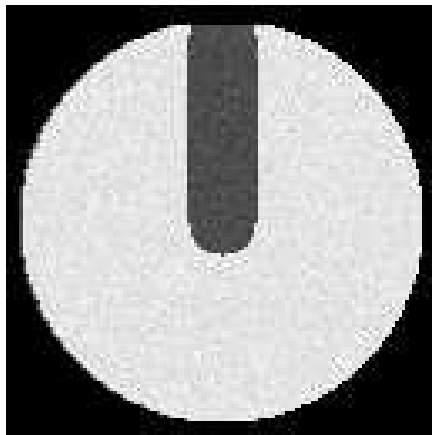
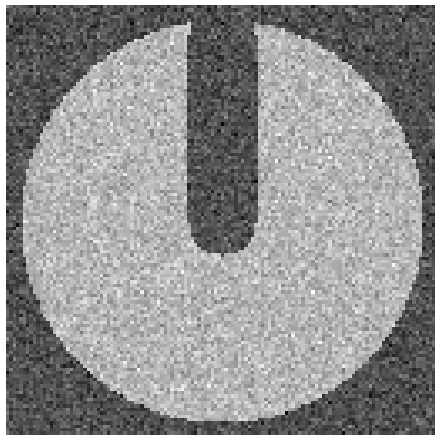


Figure 6: Phantom